Keniry, M. A., Gutowsky, H. S., & Oldfield, E. (1984a) *Nature (London) 307*, 383-386.
Keniry, M. A., Kintanar, A., Smith, R. L., Gutowsky, H. S., & Oldfield, E. (1984b) *Biochemistry 23*, 288-298.
Kim, C. H., & Hollocher, T. C. (1982) *J. Bacteriol. 151*, 358-364.
Kinsey, R. A., Kintanar, A., & Oldfield, E. (1981a) *J. Biol. Chem. 256*, 9028-9036.
Kinsey, R. A., Kintanar, A., Tsai, M.-D., Smith, R. L., James, N., & Oldfield, E. (1981a) *J. Biol. Chem. 256*, 4146-4149.
Leo, G. C., Colnago, L. A., Valentine, K. G., & Opella, S. J. (1987) *Biochemistry* (following paper in this issue).
Levitt, M., Suter, D., & Ernst, R. R. (1984) *J. Chem. Phys. 80*, 3064-3068.
Levitt, M., Suter, D., & Ernst, R. R. (1986) *J. Chem. Phys. 84*, 4243-4255.
Makowski, L. (1984) in *Biological Macromolecules and Assemblies* (McPherson, A., Ed.) pp 203-253, Wiley, New York.
Makowski, L., & Caspar, D. L. D. (1981) *J. Mol. Biol. 145*, 611-617.
Marvin, D. A., & Hohn, B. (1969) *Bacteriol. Rev. 33*, 172-209.
Nakashima, Y., & Konigsberg, W. (1974) *J. Mol. Biol. 88*, 598-600.
Oldfield, E., Kinsey, R. A., & Kintanar, A. (1982) *Methods Enzymol. 88*, 210-323.
Opella, S. J. (1986) *Methods Enzymol. 131*, 327-361.
Opella, S. J., Stewart, P. L., & Valentine, K. G. (1987) *Q. Rev. Biophys.* (in press).
Pines, A., Gibby, M., & Waugh, J. S. (1973) *J. Chem. Phys. 59*, 569-590.
Rice, D. M., Blume, A., Herzfeld, J., Wittebort, R. J., Huang, T. H., Das Gupta, S. K., & Griffin, R. G. (1981) in *Biomolecular Stereodynamics, Proceedings of the Second SUNYA Conversation in the Discipline Biomolecular Stereodynamics* (Sarma, R., Ed.) pp 255-270, Adenine, Guilderland, NY.
Schramm, S., Kinsey, R. A., Kintanar, A., Rothgeb, T. M., & Oldfield, E. (1981) in *Biomolecular Stereodynamics, Proceedings of the Second SUNYA Conversation in the Discipline Biomolecular Stereodynamics* (Sarma, R., Ed.) pp 271-286, Adenine, Guilderland, NY.
Smith, R. L., & Oldfield, E. (1984) *Science (Washington, D.C.) 225*, 280-288.
Soda, G., & Chiba, T. (1969) *J. Chem. Phys. 50*, 439-455.
Stejskal, E. O., & Schaefer, J. (1975) *J. Magn. Reson. 18*, 560-566.
Torchia, D. A. (1982) *Methods Enzymol. 82*, 174-186.
Torchia, D. A. (1984) *Annu. Rev. Biophys. Bioeng. 13*, 125-144.
Valentine, K. G., Schneider, D. M., Leo, G. C., Colnago, L. A., & Opella, S. J. (1985) *Biophys. J. 49*, 36-38.

Dynamics of fd Coat Protein in Lipid Bilayers†

G. C. Leo,‡ L. A. Colnago,§ K. G. Valentine,‖ and S. J. Opella*
Department of Chemistry, University of Pennsylvania, Philadelphia, Pennsylvania 19104
Received April 15, 1986; Revised Manuscript Received September 25, 1986

ABSTRACT: The dynamics of backbone and side-chain sites of the membrane-bound form of fd coat protein are described with solid-state ^2H and ^{15}N NMR experiments. The samples were isotopically labeled coat protein in phospholipid bilayers in excess water. The protein itself is immobile and does not undergo rapid rotation within the bilayer. Like the structural form of the protein, the membrane-bound form has four mobile residues at the N-terminus. The membrane-bound form differs from the structural form in having several mobile residues at the C-terminus. Many of the side chains of residues with immobile backbone sites undergo large amplitude jump motions. The dynamics are generally similar in both the structural and membrane-bound forms of the protein.

The major coat protein of the filamentous bacteriophages is an interesting and popular system for study because it has roles as both a membrane-bound and a structural protein during the viral life cycle (Marvin & Hohn, 1969; Makowski, 1984). We are studying the coat protein in both its membrane-bound (Cross & Opella, 1979, 1980, 1981; Frey et al., 1983; Bogusky et al., 1985a,b, 1987; Valentine et al., 1985; Colnago et al., 1986) and its structural (Opella et al., 1979, 1980; Cross et al., 1981, 1982, 1983; Cross & Opella, 1982, 1983, 1985; Gall et al., 1981, 1982; Colnago et al., 1986, 1987) forms by NMR spectroscopy. The overall goal of these investigations is to develop an understanding of the relationship between the two forms of the protein and their roles in the infection and assembly processes of the viral life cycle.

The coat protein adopts its membrane-bound conformation in the presence of a variety of lipids and detergents (Nozaki et al., 1976). Samples of the protein in detergent micelles and in sonicated phospholipid vesicles are well suited for high-resolution solution NMR studies as pursued by us (Cross & Opella, 1979, 1980, 1981; Bogusky et al., 1985a,b, 1987; Schiksuis et al., 1987) and others (Hagen et al., 1978, 1979a,b; Dettman et al., 1982, 1984; Henry et al., 1985, 1987; Wilson & Dahlquist, 1985). Samples of the protein in phospholipid bilayers are well suited for solid-state NMR studies as described here and in earlier publications (Frey et al., 1983;

† This research was supported by grants from the National Institutes of Health (GM-24266, GM-34343, and AI-20770) and by Smith Kline & French Laboratories. L.A.C. was supported by a fellowship from Conselho Nacional de Desenvolvimento Científico e tecnológico (CNPq) Brazil.
‡ Present address: Monsanto Co., St. Louis, MO 63167.
§ Present address: EMBRADA, São Carlos-S.P., 13560 Brazil.
‖ Present address: Department of Chemistry, Princeton University, Princeton, NJ 08540.

0006-2960/87/0426-0854$01.50/0

Bogusky et al., 1985a; Colnago et al., 1986; Valentine et al., 1985). These different preparations of the membrane-bound form of the coat protein enable comparisons to be made between findings from solution and solid-state NMR experiments. Since spectroscopic parameters are influenced by events on very different time scales in these two types of NMR studies, comparisons between solution and solid-state NMR results can be helpful in describing protein dynamics. Other comparisons of more biological interest are also possible from these studies, including those between the membrane-bound and structural forms of the coat protein and between the proteins from representatives of class I bacteriophages (e.g., fd, M13) and class II bacteriophages (e.g., Pf1).

Viruses, like other complex biological structures, are assembled from previously synthesized pools of constituent biopolymers (Casjens & King, 1975). The assembly pathways are of considerable interest for understanding the completed structures, as well as the flow of information and energy in biological systems. The filamentous bacteriophages undergo a complex assembly process, with the actual formation of the virus particles occurring at the bacterial cell membrane as the coat protein goes from its membrane-bound form to its structural form in the virus coat surrounding the DNA (Denhardt, 1975; Ray, 1977).

At infection, the viral DNA goes into the cell cytoplasm while the viral coat protein is inserted into the cell membrane of the bacteria (Smilowitz et al., 1972). Therefore, both the infection of the bacteria by the virus and the assembly of new virus particles involve transitions of the coat protein between the virus particle and the bacterial cell membrane. These transitions are accompanied by substantial changes in the properties of the coat protein. The transition of the coat protein in the infection process appears, at least superficially, to be the reverse of the assembly process, where the protein goes from the viral form to the membrane-bound form.

The coat protein has been studied in its membrane-bound form with a variety of methods besides NMR. Interpretations of circular dichroism and laser Raman data are consistent in suggesting that the coat protein has a large amount of secondary structure in phospholipid and detergent environments and that the membrane-bound form of the protein differs substantially from the structural form found in the virus (Chamberlain et al., 1978; Nozaki et al., 1976, 1978; Makino et al., 1978; Williams & Dunker, 1977; Fodor et al., 1981). The coat protein has a central 19-residue region of hydrophobic amino acids while the C- and N-terminal regions are relatively hydrophilic (Asbeck et al., 1969; Nakashima & Konigsberg, 1974). A model with the coat protein spanning the lipid bilayer is consistent with all of the experimental results obtained to date and seems sensible on the basis of the striking distribution of hydrophobic and hydrophilic residues in the protein.

The dynamics of the structural form of the coat protein in the virus are described in the preceding paper (Colnago et al., 1987) and elsewhere (Gall et al., 1981, 1982; Cross & Opella, 1982; Colnago et al., 1986; Valentine et al., 1985). Nearly all of the polypeptide backbone sites of the structural form of the protein are highly constrained, undergoing only small amplitude rapid motions (Cross & Opella, 1982); however, there are four highly mobile residues at the N-terminus that undergo essentially isotropic motions on the 10^3-Hz time scale (Colnago et al., 1986, 1987; Valentine et al., 1985). The side chains of many residues in the coat protein in the virus particle undergo large amplitude jump motions (Gall et al., 1981, 1982; Colnago et al., 1985, 1987; Valentine et al., 1985). This paper presents a description of the dynamics of the membrane-bound form of fd coat protein and compares the dynamics of the structural and membrane-bound forms of the protein.

Materials and Methods

Sample Preparation. The preparation of the virus is described in the preceding paper (Colnago et al., 1987). The coat protein was transferred from the virus into dimyristoyllecithin (DML) or dipalmitoyllecithin (DPL) bilayers according to the direct sonication procedure described by Fodor et al. (1981). The virus was dialyzed against distilled deionized water and then added to uniformly suspended lipids. Most samples were prepared with a slightly less than 1:1 weight ratio of protein to lipid; this corresponds to about eight lipid molecules per protein molecule and is the same high ratio used in other physical studies (Williams & Dunker, 1977). Some samples were prepared with substantially lower protein to lipid ratios in control experiments that gave results essentially the same as those reported here. The mixture was sonicated under low power with a Sonifier cell disrupter Model 350 from Branson Sonic Power Co. The temperature was maintained slightly higher than the phase-transition temperature of the pure lipid. Sonication was stopped when the solution became transparent, generally after 5–20 min depending on the sample size. The sample was then lyophilized and rehydrated with distilled deionized water. Deuterium-depleted water (Sigma) was used for the ^2H NMR experiments. The experimental samples typically contained 100–200 mg of protein.

Analytical sucrose gradients (0–60%) were used to check that the virus particles were fully disrupted and that all of the coat protein was actually associated with the lipids. The protein–lipid bands were well-defined and appeared opaque white. Fractions were monitored at 280 nm, taking into account the absorption due to the sucrose and using a small amount of sodium dodecyl sulfate (2%) to solubilize the material in the band for measurements. The complete association of the protein with lipids was also demonstrated by the finding of transparent samples following sonication, since isolated coat protein is completely insoluble in water.

Differential scanning calorimetry (DSC) indicated that there was no distinct thermotropic transition of the protein–lipid complex. ^{31}P NMR of the samples yielded axially symmetric line shapes from the phosphate head groups that are highly characteristic of intact phospholipid bilayers. There was no evidence of an isotropic ^{31}P resonance, which indicates that all of the phospholipids were in bilayers.

Enzyme Digestion. The coat protein in phospholipid bilayers was cleaved with approximately 50 μg/mL of chymotrypsin (Worthington) at 37 °C for at least 3 h in a buffer of 50 mM NH_4HCO_3 at pH 8 on samples that were about 1 mg/mL in protein. The enzyme was sonicated briefly with the protein/DML preparation. The digested fragments were separated from the core region of the protein by solubilizing aliquots of the digested protein/lipid fraction with deoxycholate (DOC) followed by precipitation with the addition of formic acid. The rest of the reaction mixture was solubilized by making the solution 8 mM in DOC; precipitation was then brought about by the addition of formic acid. The precipitate was pelleted in a Fisher microcentrifuge. The supernatant containing the fragments was injected into a Waters high-performance liquid chromatographer with a Nova Pak C-18 reverse-phase column. Isolation of the fragments was achieved by eluting the column with a linear 0–40% acetonitrile (0.1% trifluoroacetic acid) gradient run over 20 min. The isolated fragments were then subjected to amino acid analysis. The results were in agree-

(hydrophilic)
NH_3^+-ALA-GLU-GLY-ASP-PRO-ALA-LYS-ALA-ALA-PHE-ASP-SER-LEU-GLN-ALA-SER-ALA-THR-GLU-...
(hydrophobic)
...-TYR-ILE-GLY-TYR-ALA-TRP-ALA-MET-VAL-VAL-VAL-ILE-VAL-GLY-ALA-THR-ILE-GLY-ILE-...
(hydrophilic)
...-LYS-LEU-PHE-LYS-LYS-PHE-THR-SER-LYS-ALA-SER-COO⁻...

FIGURE 1: Amino acid sequence of fd coat protein (Asbeck et al., 1969; Nakashima & Konigsberg, 1974).

ment with previous chymotrypsin digests of the membrane form of the coat protein (Woolford & Webster, 1975; Dettman et al., 1982, 1984); the cleavages were found to occur after the carboxyl side of the phenylalanine residues yielding fragments 1–11, 43–45, and 46–50. Thus, the core region of the protein found in the bilayers contained the residues from Asp-12 to Phe-42.

Spectroscopy. The instrumentation and methods are described in the preceding paper (Colnago et al., 1987).

RESULTS

Backbone Dynamics. The amino acid sequence of the coat protein from fd is given in Figure 1 (Asbeck et al., 1969; Nakashima & Konigsberg, 1974). Since there is only one or a few residues of most of the amino acids in the sequence of this protein, considerable selectivity can be obtained by labeling one type of residue at a time with stable isotopes. Proteolytic cleavages of the protein offer additional selectivity (Woolford & Webster, 1975; Dettman et al., 1982, 1984).

Spectroscopic selectivity among sites can be obtained with various solid-state NMR experiments. The observable ^{15}N magnetization can be generated in solid-state NMR experiments through cross-polarization from abundant ^1H spins (Pines et al., 1973). Heteronuclear dipolar couplings are essential for cross-polarization to be effective. However, the same large amplitude, rapid motions that average the chemical shift anisotropy and quadrupole interactions as seen in the spectral line shapes also average the dipolar interactions. As a result, the sites with extensive motional averaging may not have strong enough dipolar couplings for cross-polarization to be effective. Direct pulsed excitation of ^{15}N magnetization has poor sensitivity because of the relatively low gyromagnetic ratio and long spin–lattice relaxation times (T_1) of ^{15}N; however, it does have the advantage that it is indiscriminatory with respect to the strength of the heteronuclear dipolar couplings. By comparing pulsed and cross-polarized spectra, "liquidlike" and "solidlike" spins can be distinguished in some cases.

Figure 2 presents proton-decoupled ^{15}N NMR spectra of fd coat protein in DML bilayers. In this sample, all of the protein nitrogen sites are uniformly labeled with ^{15}N. The top spectrum (Figure 2A) was obtained through direct-pulsed excitation, allowing for relaxation of the nitrogen spins during the recycle delay. The spectrum in Figure 2B was obtained by cross-polarization. Figure 2 (parts C and D) contains calculated chemical shift spectra based on representative values of the magnitudes of the principal elements of the ^{15}N amide chemical shift tensor observed in peptides and proteins. Figure 2D is a rigid lattice powder pattern with a frequency breadth of 10^3–10^4 Hz at available field strengths. Isotropic motional averaging of an amide ^{15}N site on time scales fast compared to the breadth of the powder pattern results in a single line spectrum (Figure 2C).

The experimental data in Figure 2A,B show that there are two distinct classes of amide resonances in the coat protein in bilayers, since a relatively narrow isotropic resonance is superimposed on a broad powder pattern with reasonably well-defined discontinuities. Amide sites without large amplitude motions yield the broad static powder pattern and are

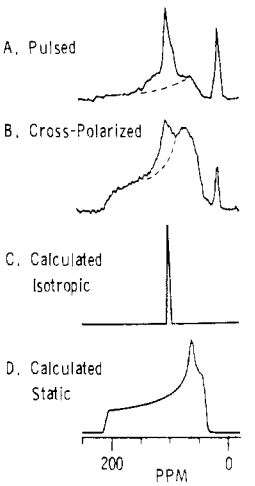

FIGURE 2: ^{15}N NMR spectra of fd coat protein in DML bilayers obtained at 25 °C. (A and B) Experimental spectra obtained on uniformly labeled coat protein. (A) was pulsed and (B) was cross-polarized. (C and D) Calculated spectra. (C) is an isotropic resonance resulting from rapid isotropic motion, and (D) is a rigid lattice powder pattern from an immobile site. The calculated spectra utilized the principal values typical of those observed in polycrystalline peptides and fd coat protein ($\sigma_{11} = -34$ ppm, $\sigma_{22} = -57$ ppm, and $\sigma_{33} = -206$ ppm) (Cross & Opella, 1985).

effectively "immobile". Motionally averaged amide sites yield the narrow resonance intensity near the amide isotropic chemical shift frequency (100 ppm). The most obvious difference between the experimental spectra obtained by direct pulsing (Figure 2A) and cross-polarization (Figure 2B) is the relative intensities of the isotropic and powder pattern resonances. The spectrum obtained by cross-polarization has a smaller contribution from the isotropic component relative to the spectrum obtained by direct pulsing, demonstrating that the development of ^{15}N magnetization by cross-polarization is influenced by the same motional averaging that affects the line shapes. The experimental spectra in Figure 2 show that some of the backbone sites are highly mobile while the majority of the amide sites are highly restrained. The line shapes and intensities of the ^{15}N NMR spectra change relatively little as a function of temperature. The ϵ-amino groups of the lysine side chains and the N-terminal alanine have small chemical shift tensors and contribute to the narrow upfield resonance near 15 ppm in the experimental spectra.

The powder pattern T_1 ($\sim$1.5 s) and nuclear Overhauser effect (NOE) ($\sim$−1) values at 25 °C indicate that small amplitude motions on the 10^9-Hz time scale are present in the otherwise immobile amide sites that give rise to the powder pattern. The presence of these rapid small amplitude motions means that the dynamics of the backbone sites contributing to the powder pattern are similar to those previously characterized for the same protein in the virus (Cross & Opella, 1982). Additional information about the backbone sites of the protein in phospholipid bilayers can be derived from ^2H NMR experiments. Figure 3 shows ^2H NMR spectra obtained from samples where the slowly exchanging amide sites on the coat protein in bilayers are labeled as N–D sites. The exchange with deuterium was performed in D_2O by raising the pH to 8.5 and the temperature to 50 °C for several hours. The sample was lyophilized after the pH was lowered to 4.0. The sample was then rehydrated with H_2O and lyophilized twice before final rehydration in deuterium-depleted water. This procedure removed the readily exchanged deuterons, which would also be the ones most likely to yield narrow isotropic resonances. The experimental spectra in Figure 3A,B are representative powder patterns for the static N–D quadrupolar

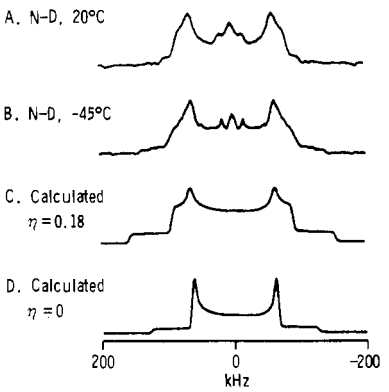

FIGURE 3: ^{2}H NMR spectra of amide N–D sites at the temperatures shown. (A and B) Experimental spectra obtained on samples of fd coat protein in DML bilayers that have been partially labeled by exchange at the amide N–D sites. (C and D) Calculated spectra. (C) is with parameters to match the experimental spectra. (D) is calculated with the same quadrupole coupling constant as in (C), although η = O.

interactions. To determine the full magnitude of the N–D quadrupole interaction in peptide bonds, the spectrum was obtained from the same sample at −45 and 20 °C (Figure 3A,B). There are only minor differences between the −45 and 20 °C spectra. These spectra are similar to those obtained from a synthetic hydrophobic peptide (Pauls et al., 1985) and from gramicidins (Datema et al., 1986) in lipid bilayers. The calculated powder patterns in Figure 3 illustrate the differences between the line shapes from the axially symmetric and nonaxially symmetric quadrupolar interactions of the same magnitude. Figure 3C is a nonaxially symmetric quadrupolar powder pattern calculated with the magnitudes of the principal values obtained from Figure 3B and from an experimental spectrum of crystalline *N*-acetylglycine. Figure 3D was calculated with the same quadrupole coupling constant as for Figure 3C but with the asymmetry parameter (η) equal to zero. The comparisons between the experimental and calculated spectra indicate that the protein itself is not reorienting within the bilayer on the 10^6-Hz time scale of the N–D quadrupole interaction. In particular, the coat protein does not undergo rapid rotation about its long axis in DML bilayers, since the nonaxially symmetric line shape of the N–D quadrupole interaction is preserved in the hydrated protein–lipid complex at 20 °C. These spectra contain some central intensity that probably results from nitrogen sites with some mobility.

Figure 4 contains ^{15}N NMR spectra of specifically ^{15}N-labeled coat proteins in DML bilayers. These data allow the protein backbone dynamics to be described with essentially atomic resolution. The four valine (29, 30, 31, and 33), two tyrosine (21 and 24), and two leucine (14 and 41) residues all yield powder patterns characteristic of highly constrained backbone sites in these spectra obtained by cross-polarization. The imide ^{15}N powder pattern for a sample labeled at Pro-6 is also characteristic of an immobile site. Immobile sites are readily observed because the powder pattern intensity can be easily obtained through cross-polarization. The spectra containing only powder patterns help define the immobile region of the protein backbone that contributes to the powder pattern observed in the heterogeneous spectrum of uniformly labeled coat protein in Figure 2B.

The ^{15}N NMR spectra from the Ala (1, 7, 9, 10, 16, 18, 25, 27, 35, and 49), Lys (8, 40, 43, 44, and 48), Gly (3, 23, 34, and 38), and Phe (11, 42, and 45) ^{15}N-labeled proteins are heterogeneous with isotropic amide resonances superimposed on powder patterns, as seen in Figure 2B for uniformly

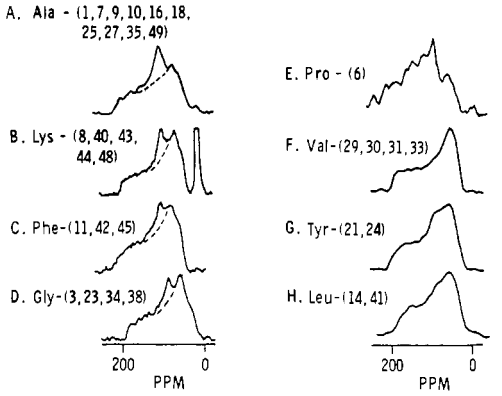

FIGURE 4: ^{15}N NMR spectra of fd coat protein in DML bilayers at 25 °C.

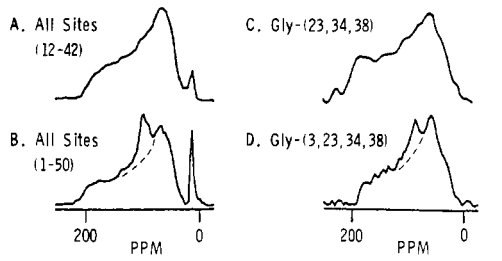

FIGURE 5: ^{15}N NMR spectra of fd coat protein in DML bilayers at 25 °C: (A and B) from uniformly ^{15}N-labeled protein; (C and D) from [^{15}N]Gly-labeled protein; (A and C) after treatment with chymotrypsin; (B and D) from intact protein.

^{15}N-labeled protein. The amide and amino resonances of the lysine-labeled protein are readily distinguished, since the narrow amino resonances are upfield near 15 ppm. The spectra in Figure 4 clearly demonstrate that there are alanine, lysine, glycine, and phenylalanine residues both in the immobile and in the mobile regions of the coat protein. These findings for proteins with only one type of labeled residue are crucial for defining the mobile regions of the protein backbone.

Treatment of coat protein samples in bilayers with chymotrypsin removes the regions encompassing residues 1–11 and 43–50 (Woolford & Webster, 1975; Dettman et al., 1982, 1984). The spectral comparisons of Figure 5 indicate that the removal of the C- and N-terminal fragments results in the loss of the isotropic amide resonance intensity in the uniformly ^{15}N-labeled and the specifically [^{15}N]Gly-labeled protein samples. The uniformly labeled protein comparison shows that all of the mobile residues are in the terminal regions of the protein that are accessible for proteolysis. The coat protein contains four glycine residues, three of which are located in the central hydrophobic region (23, 34, and 38) and one of which (3) is near the N-terminus. Since Gly-3 is the only glycine residue removed by treatment with chymotrypsin, the isotropic component in the spectrum in Figure 5D can be assigned to Gly-3. The results of Figure 5 serve to associate the mobile backbone sites with the terminal regions (1–11 and 43–50) of the protein and the rigid backbone sites with the central region (12–42) of the protein. These results supplement the findings based on the specifically labeled residues in Figure 4.

The dynamics of alanine methyl side chains can also be used to describe backbone dynamics, since the methyl group is directly bonded to the α-carbon. Any motions influencing the line shape, other than threefold methyl reorientation about the C_α–C_β bond axis, must arise from the peptide backbone (Jelinski et al., 1980; Batchelder et al., 1983; Keniry et al., 1984b). All alanine methyl groups undergo rapid threefold reorientation about the C_α–C_β bond axis at the temperatures used

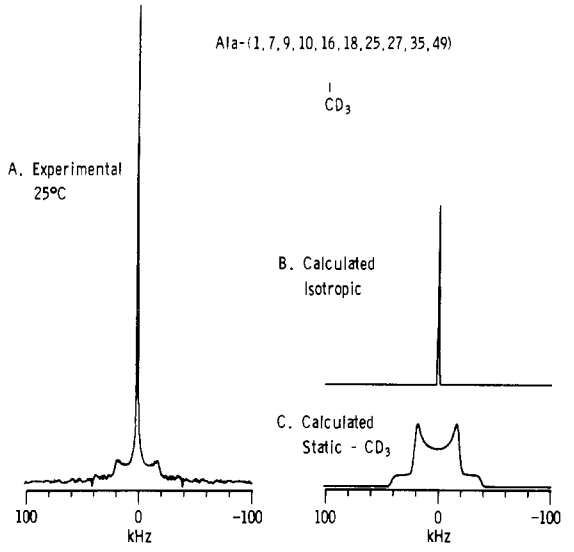

FIGURE 6: ^2H NMR spectra of CD_3 Ala labeled fd coat protein in DML bilayers.

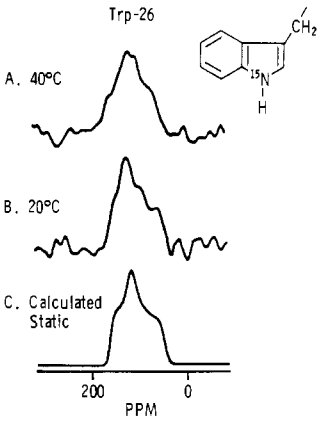

FIGURE 7: ^{15}N NMR spectra of Trp-26-labeled fd coat protein in DML bilayers.

in these experiments. Figure 6C shows a calculated ^2H NMR powder pattern for a methyl group undergoing threefold reorientation about the C_α–C_β bond axis but no other motion. Isotropic averaging results in a single-line spectrum as in Figure 6B. The experimental ^2H NMR spectrum of CD_3 Ala labeled coat protein in DML bilayers is in Figure 6A. This spectrum is clearly heterogeneous showing isotropic intensity superimposed on a methyl powder pattern. This result is consistent with that in Figure 4A for [^{15}N]Ala-labeled protein is showing mobile and immobile alanine residues in the protein.

Side-Chain Dynamics. fd coat protein has a single tryptophan residue (Trp-26). The tryptophan side chain is immobile on the NMR time scales in the structural form of the protein in the virus, as shown with ^2H, ^{13}C, and ^{15}N NMR experiments (Gall et al., 1982). The data in Figure 7 show that this side chain is also immobile in the membrane-bound form of the protein. The spectrum in Figure 7C is a calculated ^{15}N chemical shift anisotropy powder pattern for the indole nitrogen site on the basis of the magnitudes of the principal elements observed for the crystalline amino acid. The experimental data from the labeled Trp-26 side chain in the protein in bilayers are in Figure 7A,B. Within the experimental limitations of signal-to-noise ratios and line shapes, the three powder patterns in Figure 7 have the same shape and breadth. Therefore, the Trp-26 side chain of fd coat protein in bilayers can be described as immobile since it does not have large amplitude motions on the 10^3-Hz time scale. In addition

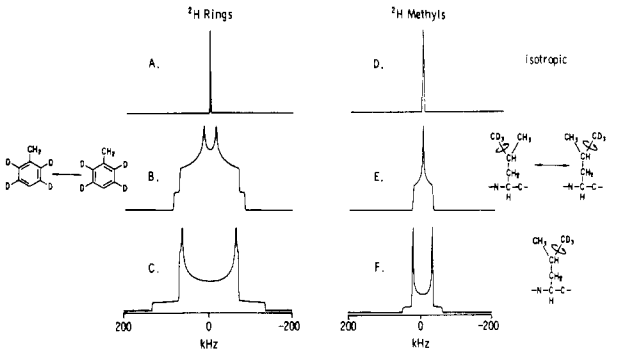

FIGURE 8: Calculated ^2H NMR powder patterns showing effects of motional averaging for phenylalanine and tyrosine side chains (A, B, and C) (Gall et al., 1982) and for Leu side chains (D, E, and F) (Colnago et al., 1987).

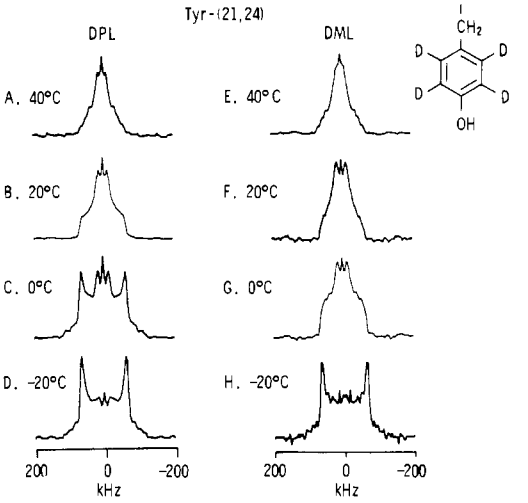

FIGURE 9: Experimental ^2H NMR spectra of [$^2H_4$]Tyr-labeled fd coat protein in phospholipid bilayers.

to demonstrating that there are no local side-chain or backbone motions at this location in the protein, the spectra in Figure 7 also show that the protein itself does not reorient within the bilayer because the nonaxially symmetric chemical shift anisotropy powder pattern line shape is present in the protein–lipid complex at 20 and 40 °C. The combination of results from Figures 3 and 7, with their characteristic nonaxially symmetric line shapes, is strong evidence that the protein itself does not rotate within the membrane bilayer.

Solid-state ^2H NMR is particularly effective in describing the dynamics of the phenyl side chains of tyrosine and phenylalanine residues in peptides and proteins (Gall et al., 1981, 1982; Rice et al., 1981a,b; Schramm et al., 1981; Gierasch et al., 1981, 1982; Oldfield et al., 1982; Frey et al., 1983, 1985a,b; Torchia, 1984; Opella, 1986). These side chains can be readily labeled in the δ- and ϵ-C–D sites synthetically or biosynthetically, and the ^2H NMR powder pattern line shapes for these sites are strongly influenced by motions about the C_β–C_γ bond axis. This can be seen in the calculated line shape comparisons in Figure 8. Twofold 180° ring flips of phenylalanine and tyrosine side chains have been observed in several proteins, including the structural form of the coat protein. Isotropically reorienting or immobile rings can also be readily identified by their ^2H NMR line shapes.

Figure 9 contains experimental ^2H NMR spectra from [$^2H_4$]Tyr-labeled coat protein in DML and in DPL bilayers. Spectral comparisons as a function of temperature and chain length of the lipids are shown. In the temperature range −20 to 20 °C, the motionally averaged experimental line shapes (Figure 9B,C,F,G) are similar to those calculated for phenyl

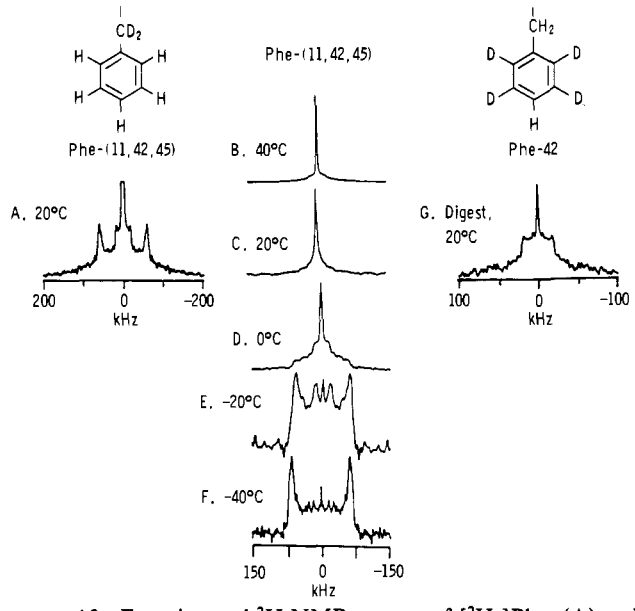

FIGURE 10: Experimental ^2H NMR spectra of [$^2H_2$]Phe- (A) and [$^2H_4$]Phe-labeled (B–G) fd coat protein in DML bilayers. The spectrum in G is from chymotrypsin-treated fd coat protein.

rings that either are immobile or are undergoing twofold jumps (Figure 8B). At higher temperatures additional motions are present, since some rounding and narrowing of the powder pattern line shapes are observed. At −20 °C, the tyrosine rings are immobile in both lipids.

The dynamics of most of the protein sites are quite similar in various lipids. However, one of the clearest differences we have observed in protein dynamics as a function of lipid can be seen in the comparison of the spectra in Figure 9 (parts C and G). In the lipid environment of DML (C_{14}), both tyrosines appear to be flipping at 0 °C, while in DPL (C_{16}) at the same temperature one ring is static and the other is flipping. At all of the temperatures used in the experiments, including 40 °C, the ^{15}N NMR spectrum of the Tyr-labeled sites is a powder pattern (Figure 4G) indicative of immobile backbone sites. The flip-averaged side-chain powder patterns also demonstrate that the backbone is rigid at these sites.

Both ^2H and ^{15}N NMR spectra show that the coat protein in lipid bilayers has at least one phenylalanine residue with a mobile backbone site and at least one with an immobile backbone site. Figure 4C shows the presence of isotropic resonance intensity from one or two mobile Phe sites superimposed on the powder pattern from one or two immobile Phe sites. The ^2H NMR spectrum in Figure 10A from CD_2 β labeled Phe sites shows that at least one of the Phe residues has a mobile backbone site, since C_β sites are directly attached to the backbone. The relative intensities of both Figure 4C and Figure 10A are not reliable in distinguishing between one or two mobile Phe backbone sites, because in both experiments the narrow isotropic resonances behaves differently from the broad powder pattern resonance intensity.

The spectra in Figure 10B–G were obtained from [$^2H_4$]-Phe-labeled coat protein. The temperature dependence of the three Phe side chains is shown in Figure 10B–F. At −40 °C, all three rings are immobile. At −20 °C, a pattern resulting from rings undergoing 180° flips and immobile rings is seen. In the spectra above 0 °C, large amounts of additional motional averaging are present. Because of the difficulties of comparing intensities of broad and narrow components, it is not possible to quantitatively interpret the side-chain data. However, it is clear that at least one of the Phe rings undergoes effectively isotropic motion under the same conditions where at least one mobile Phe backbone site was observed in the data of Figures 4C and 10A. The spectrum in Figure 10G of [$^2H_4$]Phe-labeled coat protein after proteolytic cleavage arises from only Phe-42, since Phe-10 and Phe-45 have been removed. This spectrum indicates that the Phe-42 ring does not undergo isotropic reorientation even though it is now the C-terminal residue of the cleaved protein. This suggests that the Phe-42 backbone is immobile in the intact protein and contributes to the powder pattern intensity in the spectra in Figures 4C and 10A.

The motions of methyl groups in aliphatic side chains reflect those of backbone and methylene sites of these residues. Methyl group motions are readily characterized by ^2H NMR studies at CD_3-labeled sites (Jelinski et al., 1980; Batchelder et al., 1982, 1983; Kinsey et al., 1981a,b; Keniry et al., 1984a,b; Smith & Oldfield, 1984; Colnago et al., 1986, 1987). In spite of the possibility of many motions in long aliphatic side chains, only a few modes of motion have been observed in solid-state NMR studies, such as those shown in Figure 8.

Both leucines in the protein have immobile peptide bonds since a ^{15}N amide powder pattern is observed in Figure 4H. The ^2H NMR spectra in Figure 11A–D show that these side

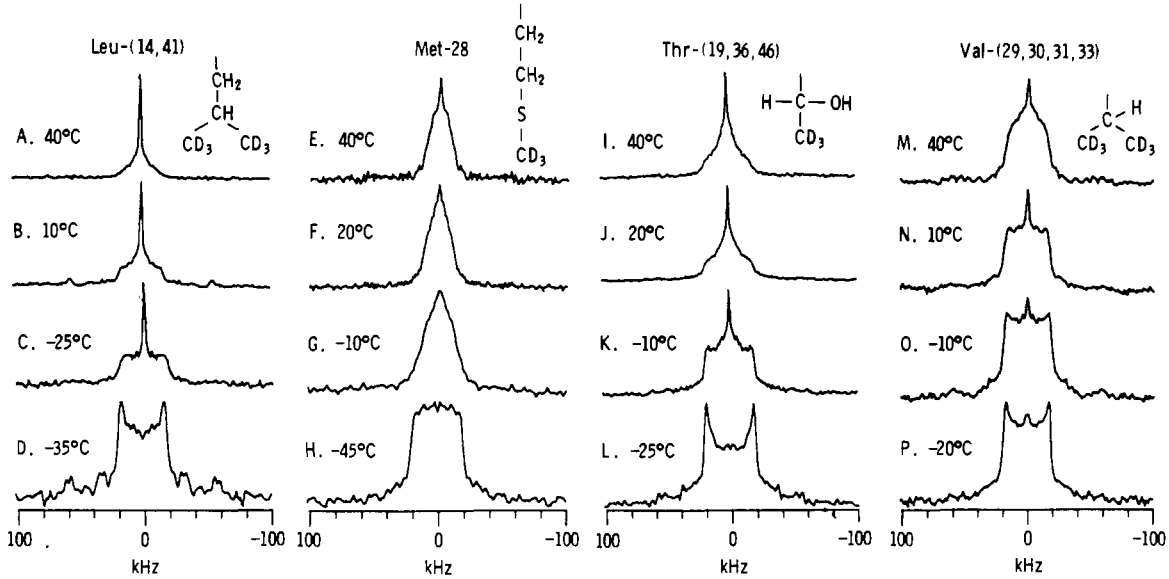

FIGURE 11: ^2H NMR spectra of CD_3-labeled sites on fd coat protein in DML as a function of temperature.

chains undergo twofold tetrahedral jump motions at temperatures above about 10 °C and only three fold methyl group reorientation at temperature below −35 °C. There are intermediate temperatures where only one of the leucines undergoes the jump motions. The line shape shows additional narrowing at higher temperatures, indicative of one or both the Leu side chains having motions in addition to two-site jumps.

The coat protein has a single methionine residue (Met-28). Therefore, when this residue is labeled biosynthetically, the line shape from the CD_3 site can be analyzed without interference from overlapping patterns.

The ^2H NMR spectra in Figure 11E–H show that only limited motional averaging occurs in this side chain. The experimental spectrum obtained at −10 °C is very similar to that calculated for twofold jumps about the S–C bond and threefold reorientation of the CD_3 group. At higher temperatures, some additional narrowing and rounding of the jump-averaged pattern is observed, indicative of limited motions about additional bonds in the side chain.

The coat protein has three threonine residues, one of which is near the C-terminus (Thr-46). The ^2H NMR spectra of the CD_3 Thr labeled protein in DML bilayers in Figures 11I–L show that these groups undergo only threefold reorientation at −25 °C. At temperatures higher than about 25 °C, all three threonine side chains undergo twofold tetrahedral jumps. The spectra suggest that one of the residues has a mobile side chain at the higher temperatures. The −10 °C spectrum shows that the threonine side chains differ in their activation energy for the large amplitude jump motion.

The four valine residues are in close proximity in the central hydrophobic region of the protein. The ^{15}N NMR spectrum in Figure 4F shows that all four have immobile peptide linkages.

The ^2H NMR spectra in Figure 11M–P indicate that the side chains have different mobilities. At low temperatures, only threefold CD_3 group reorientation is observed. At 10 °C, the spectrum appears to be a superposition of powder patterns resulting from tetrahedral jump motions and the methyl group reorientation. At 40 °C the pattern is more complex, indicating the presence of additional types of motion in the side chains. The small central resonance signal that is present at all temperatures is unlikely to be a contribution from a valine side chain undergoing isotropic motion.

Discussion

The preceding paper (Colnago et al., 1987) summarized our current level of understanding of the dynamics of the structural form of the coat protein in the bacteriophage. In its structural form, the coat protein has four highly mobile residues at the N-terminus. The rest of the backbone of the protein in the virus is highly constrained, although small amplitude motions are present. Most of the amino acid side chains undergo large amplitude rapid motions in the form of jumps about single carbon bonds; these are 180° ring flips about the C_β–C_γ for Phe and Tyr and hops about tetrahedral or near-tetrahedral carbon sites in aliphatic side chains. Nearly all of the experimental line shapes are well simulated by line shapes calculated on the basis of models with only one or two modes of motion.

The membrane-bound form of the coat protein differs from the structural form in that the backbone sites of more residues undergo isotropic motion in the membrane-bound form. The pattern of side-chain motions is generally similar in the two forms; however, in many cases small amounts of additional motional averaging cause additional narrowing of the powder patterns in the membrane-bound form.

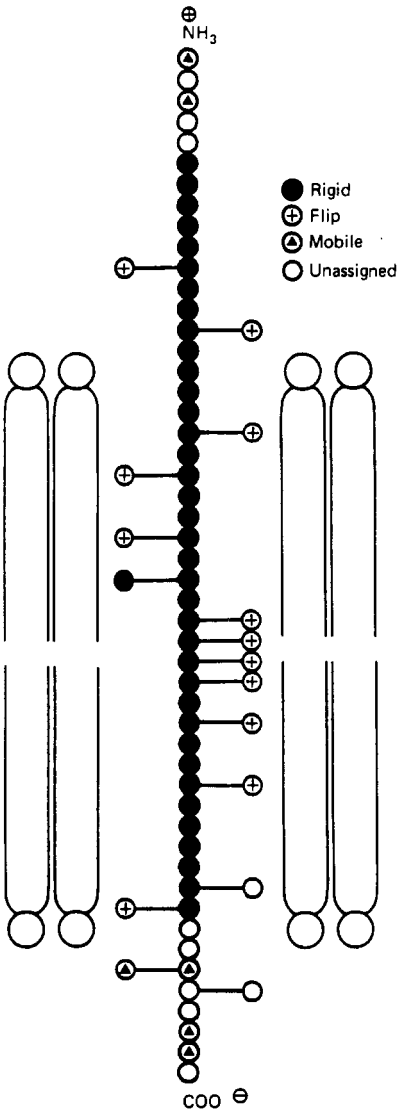

FIGURE 12: Summary of dynamics of fd coat protein in phospholipid bilayers.

The major change in the coat protein when it goes from the structural form in the virus to the membrane-bound form is that several C-terminal residues go from being rigidily constrained in the virus particle to highly mobile in the membrane-bound form. As shown in Figure 12, the backbone of the protein from residue 5 or 6 through residue 42 or 43 is immobile. This contrasts with the structural form of the coat protein in the virus where residues 5–50 have immobile backbone sites.

The ^{15}N NMR spectrum in Figure 5A demonstrates that residues 12–42 have immobile backbone sites. The ^{15}N NMR spectra in Figure 4E–H show that the region includes residues 6–41. The spectra with narrow isotropic resonances from mobile sites superimposed on powder patterns from rigid sites demonstrate that a limited number of residues are highly mobile. The specific labeling of the Gly residues and the spectra obtained of the intact protein and the protein with residues 12–42 following proteolysis demonstrate that Gly-3 is mobile and that the other three Gly residues (23, 24, and 38) are immobile. The ^{15}N NMR spectrum of Ala-labeled protein indicates that at least one Ala residue, in addition ot the *N*-terminal Ala, is mobile, since the *N*-terminal amino group gives the upfield resonance near 15 ppm and the mobile Ala amide group gives the isotropic resonance near 100 pm

in Figure 4A. The ^2H NMR spectrum of CD_3-labeled Ala also shows that one or more Ala residues have isotropic motion but that many of them are immobile.

The powder pattern obtained for the ^{15}N resonance from Pro-6 indicates that this site is rigid. Therefore, Ala-7 must also be immobile. Ala-1 is mobile on the basis of Gly-3 being mobile. Ala-35 is immobile because after proteolysis residues 12–42 remain and none of them are mobile and the specific site labeled proteins show that nearby residues such as Val-31, Val-33, Gly-34, and Gly-38 are immobile. Therefore, Ala-49 is mobile and is the sole source of the isotropic ^{15}N amide intensity in Figure 4A and contributes along with Ala-1 to the isotropic ^2H resonance intensity in Figure 6A. This establishes that several N-terminal residues of the membrane-bound form of the coat protein are mobile, since Ala-1 and Gly-3 are mobile and Pro-6 is immobile. Four N-terminal residues were found to be mobile in the structural form of the coat protein in the virus (Colnago et al., 1987). Therefore, the dynamics of the N-terminus appears to be the same in both forms of the protein.

The next point of discussion concerns how many mobile C-terminal residues are present in the membrane-bound form of the coat protein. Leu-41 is immobile on the basis of the ^{15}N NMR spectrum in Figure 4H, and Phe-42 is immobile on the basis of the spectrum in Figure 5A of the uniformly labeled protein following proteolysis and the corresponding ^2H NMR spectrum in Figure 10G; therefore, there are at most eight mobile C-terminal residues.

Since residue 6 is immobile, Lys-8 and Phe-11 must also be immobile. However, the spectra in Figure 4 (parts B and C) demonstrate the presence of mobile Lys and Phe residues. Phe-45 must be mobile to account for the isotropic resonance intensity in Figures 4C and 10A, since Phe-11 and Phe-42 are immobile on the basis of the arguments given above. There are five Lys residues, and at least two of them (Lys-8 and Lys-40) have immobile backbone sites by the reasoning used to this point, and one or more Lys residues are mobile on the basis of the ^{15}N NMR spectrum in Figure 4B. The data presented here do not establish the definitive breakpoint between mobile and immobile C-terminal residues. Some powder pattern and magic angle spinning spectra of the [^{15}N]Lys-labeled coat protein in bilayers show evidence of resolution of the isotropic resonance into two components, suggesting that Lys-44 is mobile in addition to Lys-48. The C-terminal residues starting with Lys-43 or Lys-44 are mobile in the membrane-bound form of the coat protein.

The finding of mobile residues near both the N- and C-termini of the coat protein in phospholipid bilayers by solid-state NMR is in qualitative agreement with the results for the coat protein in detergent micelles by solution NMR (Cross & Opella, 1980, 1981; Bogusky et al., 1985a,b, 1987). In particular, Henry et al. (1986) found both Ala-1 and Ala-49 but not the other alanine residues to be highly mobile in the coat protein in micelles.

Earlier discussions (Frey et al., 1983; Colnago et al., 1986) of the dynamics of the Phe residues in the membrane-bound form focused on ^2H NMR spectra as in Figure 10B, which seem to indicate that all three have highly mobile side chains. The recent implementation of the phase-alternated cross-polarization method (Levitt et al., 1986) has yielded ^{15}N NMR spectra as in Figure 4C, which clearly show that the Phe residues have heterogeneous dynamics. The earlier models of the backbone dynamics of the protein in bilayer had more mobile sites than the current model shown in Figure 12 because of the experimental results for the Phe residues.

The side-chain dynamics in the two forms of the coat protein are generally similar with either rigidly held groups, such as Trp-26 in both forms, or side chains undergoing jump motions, such as the Tyr-21 and Tyr-24 or Leu-14 and Leu-41. However, in many cases there is evidence for the presence of additional motions in the membrane-bound form as seen in rounding of powder patterns and additional central intensity. The nature of smaller amplitude motions remains to be described in studies of proteins with only a single labeled side chain.

ACKNOWLEDGMENTS

We thank J. DiVerdi for help with the NMR spectroscopy carried out at Smith Kline & French Laboratories, S. Fodor for helpful discussions, B. Bachmann for supplying the *E. coli* Pro auxotroph, and M. Levitt, E. Oldfield, and B. Sykes for providing preprints of their work.

Registry No. DML, 13699-48-4; DPL, 2644-64-6.

REFERENCES

Asbeck, F., Beyreuther, K., Kohler, H., Von Wettstein, G., & Braunitzer, G. (1969) *Hoppe-Seyler's Z. Physiol. Chem. 350*, 1047–1066.

Batchelder, L. S., Sullivan, C. P., Jelinski, L. W., & Torchia, D. A. (1982) *Proc. Natl. Acad. Sci. U.S.A. 79*, 386–389.

Batchelder, L. S., Niu, C. H., & Torchia, D. A. (1983) *J. Am. Chem. Soc. 105*, 2228–2231.

Bogusky, M. J., Leo, G. C., & Opella, S. J. (1985a) in *Magnetic Resonance in Biology and Medicine* (Govil, Khetrapal, & Saren, Eds.) pp 375–383 Tata McGraw-Hill, New Delhi.

Bogusky, M. J., Tsang, P., & Opella, S. J. (1985b) *Biochem. Biophys. Res. Commun. 127*, 540–545.

Bogusky, M. J., Schiksuis, R. A., & Opella, S. J. (1987) *J. Magn. Reson.* (in press).

Casjens, S., & King, J. (1975) *Annu. Rev. Biochem. 44*, 555–612.

Chamberlain, B. K., Nozaki, Y., Tanford, C., & Webster, R. E. (1978) *Biochim. Biophys. Acta 510*, 18–37.

Colnago, L. A., Leo, G. C., Valentine, K. G., & Opella, S. J. (1986) in *Biomolecular Stereodynamics, Proceedings of the Fourth SUNYA Conversation in the Discipline Biomolecular Stereodynamics* (Sarma, R. H., & Sarma, M. H., Eds.) Vol. III, pp 147–158, Adenine, Guilderland, NY.

Colnago, L. A., Valentine, K. G., & Opella, S. J. (1987) *Biochemistry* (preceding paper in this issue).

Cross, T. A., & Opella, S. J. (1979) *J. Supramol. Struct. 11*, 139–145.

Cross, T. A., & Opella, S. J. (1980) *Biochem. Biophys. Res. Commun. 92*, 478–484.

Cross, T. A., & Opella, S. J. (1981) *Biochemistry 20*, 290–297.

Cross, T. A., & Opella, S. J. (1982) *J. Mol. Biol. 159*, 543–549.

Cross, T. A., & Opella, S. J. (1983) *J. Am. Chem. Soc. 105*, 306–308.

Cross, T. A., & Opella, S. J. (1985) *J. Mol. Biol. 182*, 367–381.

Cross, T. A., Gall, C. M., & Opella, S. J. (1981) in *Progress in Clinical and Biological Research* (DuBow, M. S., Ed.) Vol. 64, pp 457–465, Liss, New York.

Cross, T. A., DiVerdi, J. A., & Opella, S. J. (1982) *J. Am. Chem. Soc. 104*, 1759–1761.

Cross, T. A., Tsang, P., & Opella, S. J. (1983) *Biochemistry 22*, 721–726.

Datema, K. P., Pauls, K. P., & Bloom, M. (1986) *Biochemistry 25*, 3796–3803.

Denhardt, D. T. (1975) *CRC Crit. Rev. Microbiol. 4*, 161–223.
Dettman, H. D., Weiner, J. H., & Sykes, B. D. (1982) *Biophys. J. 37*, 243–251.
Dettman, H. D., Weiner, J. H., & Sykes, B. D. (1984) *Biochemistry 23*, 705–712.
Fodor, S. P. A., Dunker, A. K., Ng, Y. C., Carsten, D., & Williams, R. W. (1981) in *Bacteriophage Assembly* (DuBow, M. S., Ed.) pp 441–455, Liss, New York.
Frey, M. H., Hexem, J. G., Leo, G. C., Tsang, P., Opella, S. J., Rockwell, A. L., & Gierasch, L. M. (1983) in *Peptides: Structure and Function, Proceedings of the Eighth American Peptide Symposium* (Hruby, V. J., & Rich, D. H., Eds.) pp 763–771, Pierce Chemical Co., Rockford, IL.
Frey, M. H., DiVerdi, J. A., & Opella, S. J. (1985a) *J. Am. Chem. Soc. 107*, 7311–7315.
Frey, M. H., Opella, S. J., Rockwell, A. L., & Giersch, L. M. (1985b) *J. Am. Chem. Soc. 107*, 1946–1951.
Gall, C. M., DiVerdi, J. A., & Opella, S. J. (1981) *J. Am. Chem. Soc. 103*, 5039–5043.
Gall, C. M., Cross, T. A., DiVerdi, J. A., & Opella, S. J. (1982) *Proc. Natl. Acad. Sci. U.S.A. 79*, 101–105.
Gierasch, L. M., Opella, S. J., & Frey, M. H. (1981) in *Peptides: Synthesis, Structure, and Function, Proceedings of the Seventh American Peptide Symposium* (Rich, D. H., & Gross, E., Eds.) pp 267–275, Pierce Chemical Co., Rockford, IL.
Gierasch, L. M., Frey, M. H., Hexem, J. G., & Opella, S. J. (1982) *ACS Symp. Ser. No. 191*, 233–247.
Hagen, D. S., Weiner, J. H., & Sykes, B. D. (1978) *Biochemistry 17*, 3860–3866.
Hagen, D. S., Weiner, J. H., & Sykes, B. D. (1979a) *Biochemistry 18*, 2007–2012.
Hagen, D. S., Weiner, J. H., & Sykes, B. D. (1979b) in *NMR and Biochemistry* (Opella, S. J., & Lu, P., Eds.) pp 51–57, Marcel Dekker, New York.
Henry, G. D., Weiner, J. H., & Sykes, B. D. (1986) *Biochemistry 25*, 590–598.
Henry, G. D., O'Neill, J. D. J., Weiner, J. H., & Sykes, B. D. (1986) *Biophys. J. 49*, 329–331.
Jelinski, L. W., Sullivan, C. E., & Torchia, D. A. (1980) *Nature (London) 284*, 531–534.
Keniry, M. A., Gutowsky, H. S., & Oldfield, E. (1984a) *Nature (London) 307*, 383–386.
Keniry, M. A., Kintanar, A., Smith, R. L., Gutowsky, H. S. & Oldfield, E. (1984b) *Biochemistry 23*, 288–298.
Kinsey, R. A., Kintanar, A., & Oldfield, E. (1981a) *J. Biol. Chem. 256*, 9028–9036.
Kinsey, R. A., Kintanar, A., Tsai, M.-D., Smith, R. L., James, N., & Oldfield, E. (1981b) *J. Biol. Chem. 256*, 4146–4149.
Levitt, M. H., Suter, D., & Ernst, R. R. (1986) *J. Chem. Phys. 84*, 4243–4255.
Makino, S., Reynolds, J. A., & Tanford, C. (1978) *J. Biol. Chem. 248*, 4926.
Makowski, L. (1984) in *Biological Macromolecules and Assemblies* (McPherson, A., Ed.) pp 203–252, Wiley, NY.
Marvin, D. A., & Hohn, B. (1969) *Bacteriol. Rev. 33*, 172–209.
Nakashima, Y., & Konigsberg, W. (1974) *J. Mol. Biol. 88*, 598–600.
Nozaki, Y., Chamberlain, B. K., Webster, R. E., & Tanford, C. (1976) *Nature (London) 259*, 335–337.
Nozaki, Y., Reynolds, J. A., & Tanford, C. (1978) *Biochemistry 178* 1239–1246.
Oldfield, E., Kinsey, R. A., & Kintanar, A. (1982) *Methods Enzymol. 88*, 210–323.
Opella, S. J. (1986) *Methods Enzymol. 131*, 327–361.
Opella, S. J., Frey, M. H., & Cross, T. A. (1979) *J. Am. Chem. Soc. 101*, 5856–5857.
Opella, S. J., Cross, T. A., DiVerdi, J. A., & Sturm, C. F. (1980) *Biophys. J. 32*, 531–548.
Pauls, K., MacKay, A., Soderman, O., Bloom, M., Tanjea, A., & Hodges, R. (1985) *Eur. Biophys. J. 12*, 1–11.
Pines, A., Gibby, M., & Waugh, J. S. (1973) *J. Chem. Phys. 59*, 569–590.
Ray, D. S. (1977) *Compr. Virol. 7*, 105.
Rice, D. M., Blume, A., Herzfeld, J., Wittebort, R. J., Huang, T. H., Das Gupta, S. K., & Griffin, R. G. (1981a) in *Biomolecular Stereodynamics, Proceedings of the Second SUNYA Conversation in the Discipline Biomolecular Stereodynamics* (Sarma, R., Ed.) Vol, II, pp 255–270, Adenine, Guilderland, NY.
Rice, D. M., Wittebort, R. J., Griffin, R. G., Meirovitch, E., Stimson, E. R., Meinwald, Y. C., Freed, J. H., & Scheraga, H. A. (1981b) *J. Am. Chem. Soc. 103*, 7707–7710.
Schiksuis, R. A., Bogusky, M. J., Tsang, P., & Opella, S. J. (1987) *Biochemistry* (in press).
Schramm, S., Kinsey, R. A., Kintanar, A., Rothgeb, T. M., & Oldfield, E. (1981) *Biomolecular Stereodynamics, Proceedings of the Second SUNYA Conversation in the Discipline Biomolecular Stereodynamics* (Sarma, R., Ed.) Vol. II, pp 271–286, Adenine, Guilderland, NY.
Smilowitz, H., Carson, J., & Robbins, P. W. (1972) *J. Supramol. Struct. 1*, 8–18.
Smith, R. L., & Oldfield, E. (1984) *Science (Washington, D.C.) 225*, 280–288.
Torchia, D. A. (1984) *Annu. Rev. Biophys. Bioeng. 13*, 125–144.
Valentine, K. G., Schneider, D. M., Leo, G. C., Colnago, L. A., & Opella, S. J. (1985) *Biophys. J. 49*, 36–38.
Williams, R., & Dunker, A. K. (1977) *J. Biol. Chem. 252*, 6253–6255.
Wilson, M. L. & Dahlquist, F. W. (1985) *Biochemistry 24*, 1920–1928.
Woolford, J. L., & Webster, R. E. (1975) *J. Biol. Chem. 250*, 4333–4339.